doi: 10.56761/EFRE2022.S6-O-010005

# Numerical simulation of individual cell of the electron beam source with a plasma cathode

*V.T. Astrelin[1,*], I.V. Kandaurov[1], V.P. Tarakanov[2]*

[1]*Budker Institute of Nuclear Physics SB RAS, Novosibirsk, Russia*
[2]*Joint Institute for High Temperatures, Moscow, Russia*
[*]*Astrelin@inp.nsk.su*

**Abstract.** In two-dimensional axisymmetric geometry, the "particles in cells" method is used to numerically simulate the elementary cell of a multi-aperture source of an electron beam based on a plasma cathode. The influence of the density of the cathode plasma and its potential on the transition from the regime of layered emission limitation to the regime of emission from an open plasma boundary is studied. The characteristics of the generated electron beam are obtained.
**Keywords:** electron beam, plasma electron emitter, ion layer, numerical simulation, KARAT.

## 1. Introduction

Electron sources based on plasma emitters have been developed and used for scientific and practical purposes since the last century and up to the present (see review [1]). Numerous studies have made it possible to obtain a qualitative and semi-quantitative physical picture of the processes for various regimes of electron emission from plasma. The quantitative calculation of electron sources was difficult due to the lack of available codes adequate to the problem. Sometimes, for this aim, programs for calculating ion beams were used with the replacement of charges and masses of ions by electronic ones [2, 3, etc.]. In them, as well as in existing codes for modeling plasma emission sources of electrons, for example [4, 5], it is assumed that electron emission occurs from an open plasma boundary. But, as a rule, in real sources of beams, an elementary emission aperture (a cell of a metal cathode grid, an emission hole in the cathode electrode, etc.) operates under conditions of limitation of electron emission by a potential barrier [1, p.46]. The barrier arises when the potential of the electrode inside the aperture is not completely screened by the plasma. In existing numerical simulation codes, this mode is usually not considered.

In this paper, to simulate plasma sources of electrons (PES) operating in different modes, the "particles in cells" method implemented in the KARAT code [6] is used. The aim of this work is to obtain a more detailed quantitative description of PES with real electrode geometry. The parameters of the used model are close to the real ones within the restrictions of the computational code, the statistics are improved. The operation of the emitter in the transition region from the regime with limited emission by a potential layer to the regime of an open plasma boundary is studied, as well as the effect of the plasma potential on the emission regime.

## 2. Multi-aperture electron beam source

For a number of years, the INP SB RAS has been studying the formation of an electron beam in a plasma-electron source (Fig.1a) with a multi-aperture EOS of the diode type [7]. On the flat electrodes of the diode, 241 holes were drilled in a hexagonal order (Fig.1b). The plasma inside the cavity of the cathode electrode was created by an arc discharge generator in a diverging magnetic field. The discharge current flowed between the cold arc cathode located inside the generator and the inner surface of the hollow cathode electrode.

Each pair of holes located coaxially on the cathode and anode electrodes formed an elementary accelerating cell. The cell draught of one of the variants of the diode assembly is shown in Fig.2. The entire beam source was in a leading magnetic field of ~ 100 G in the region of the diode and 2–5 kG in the region of the arc generator. The diode gap voltage could vary within $U_a$ = 40–100 kV, and the total emission current extracted from the cathode plasma was $I_b$ ~ 10–100 A.

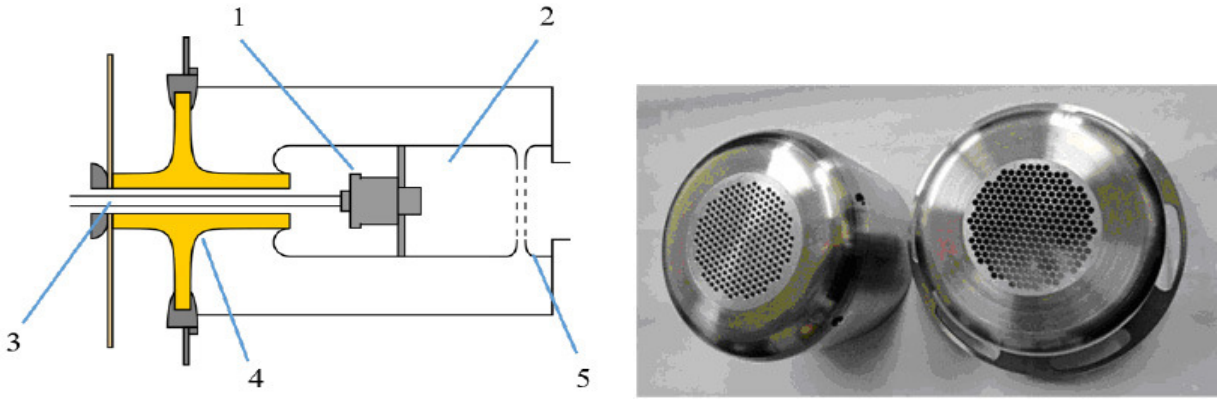


(a) (b)

Fig.1. a) Diagram of the beam source: arc plasma generator (1); plasma expander (hollow arc anode) (2); generator power supply and gas supply (3); high voltage insulator (4); extracting electrode (diode anode) (5); b) source cathode (left) and anode (right) [7].

The main problem in formulating the problem is the lack of data on the parameters of the emission plasma. Therefore, parameters typical for such emitters [1] are used in the model.

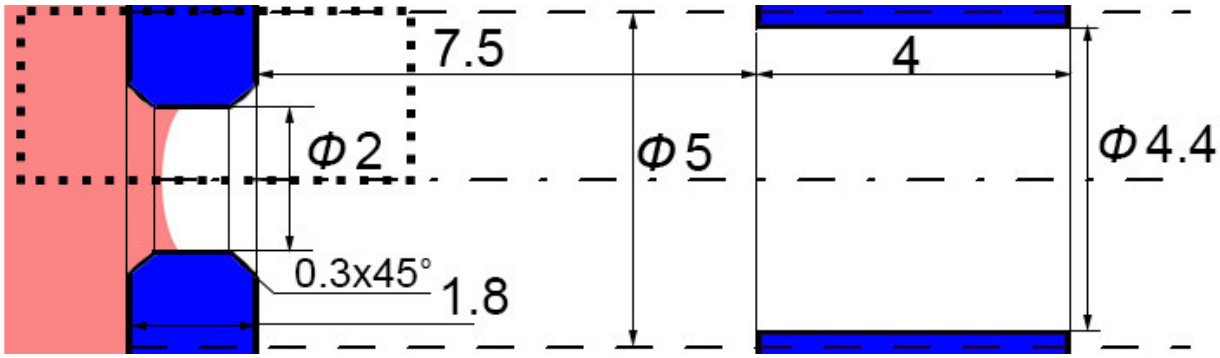


Fig.2. A diode cell. On the left is the cathode with plasma, on the right is the anode. The dotted line is the periodicity boundary. The dots mark the simulation area. Dimensions are in millimeters.

We consider a hydrogen plasma with a density $n_0 = 10^9$–$10^{11}$ cm$^{-3}$, temperature of electrons $T_e = 10$ eV and ions $T_i = 1$ eV. The plasma potential is established in the system, which is determined by the balance of currents entering and leaving the plasma. In the absence of currents external to the source, the floating plasma potential $\varphi_p$ is determined by the condition $I_e = I_i$, or

$$I_e = j_e S = en_0 S\sqrt{T_e/2\pi m}\cdot\exp(-\varphi_p/T_e) = I_i \sim j_B S = 0.6en_0 S\sqrt{T_e/M} \qquad (1)$$

in standard notation. Here $j_B$ is the Bohm ion current density for $T_i \ll T_e$ and $S$ is the plasma surface. For the plasma under consideration, the floating potential is equal to

$$\varphi_p = T_e \ln\left[0.6\left(M/2\pi m\right)^{1/2}\right] \approx 3.35T_e . \qquad (2)$$

The currents of the external circuit, including the emission current from the plasma, can change its potential. It may also depend on the magnetic field inside the cathode, which affects the contact of the plasma with the wall. These factors are not taken into account in the model. Therefore, to study the effect of the plasma potential on electron emission, we will vary its value in the region of the floating potential.

## 3. Numerical model of the emitter

The operation of the plasma emitter is analyzed by the PIC method [6]. The simulation area is highlighted in Fig.2 by dots and shown separately in Fig.3. A two-dimensional axis-symmetric problem is being solved in $r$-$z$ coordinates. The computational area is divided by the cathode electrode into two parts. The left side is the volume inside the cathode filled with plasma. The right one is the region of electron acceleration. The cathode electrode with zero potential is located at $3 < z < 4.8$ mm, its lower edge with chamfers forms an aperture with a radius $r_0 = 1$ mm. On the left boundary of the region, a plasma flow source with a potential $U_p = 30$ V, close to the floating plasma potential $\varphi_p$, is set. At the upper boundary, a periodic boundary condition with period of 5 mm is simulated.

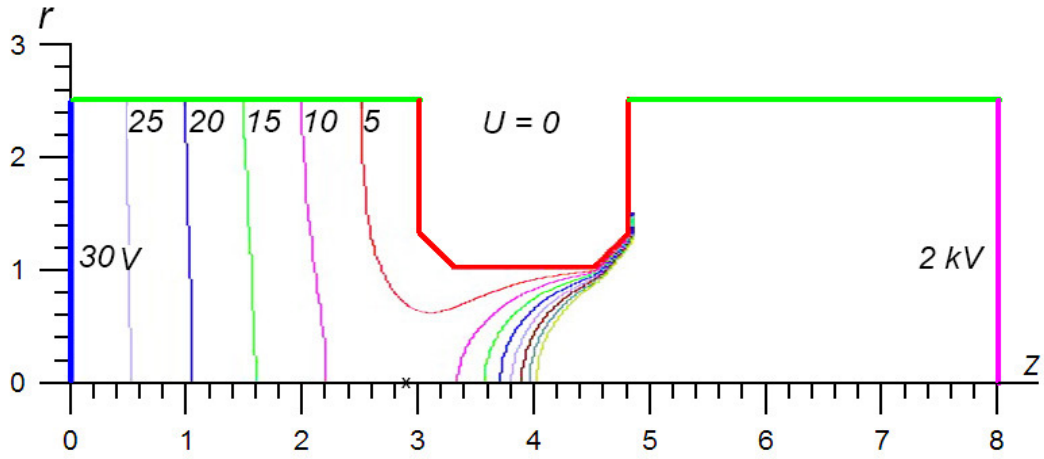


Fig.3. The computational domain of the simulated system and the map of equipotentials in the absence of particle flows. Coordinates are in millimeters. A saddle point is marked with a cross on the axis.

Fig.3 shows a map of equipotential lines in the absence of plasma flows. The potential of the right boundary $U = 2$ kV is set, which approximately corresponds to the anode potential $U_a = 4.7$ kV. With it, a stable convergence of code algorithms is still observed, and with an increase in the potential, the convergence deteriorates sharply. In this configuration, a saddle-shaped potential profile $U(r, z)$ arises with a saddle point $U_s \sim 7$ V at $z_s \sim 2.9$ mm. For plasma electrons, this corresponds to a potential barrier dropping from 30 eV at the cathode electrode to a minimum $w_e \sim 23$ eV at the axis.

The plasma filling the cathode volume is modeled by the heat fluxes of macroparticles corresponding to electrons and protons emerging from the left boundary. Plasma components with a uniform flow distribution along the $r$-coordinate have a Maxwellian isotropic distribution of particle velocities in the direction transverse to the $z$ axis. A semi-Maxwellian distribution is specified for electrons and ions along the axis, and the drift energy $w_B = 5$ eV corresponding to the Bohm velocity is added to the $z$-component of the thermal energy of ions. The problem of the formation of plasma layers and particle flows in self-consistent electric fields is solved dynamically by establishing the system parameters in time until a steady state is reached.

The choice of plasma parameters takes into account both the problem being solved and the limitations of the numerical code. The ion density of the plasma is chosen such as to obtain the regime of layered emission stabilization and the regime of an open plasma boundary. In this case, the minimum ion density is such that it sets the Debye length that is a multiple times less of the gap between the left boundary of the computational region and the cathode electrode, but comparable to the radius of the emission aperture. The maximum ion density is limited by the Debye length, which is a multiple times greater of the computational grid step, by statistical noise, and the convergence

of numerical algorithms. The correctness of the setting of the electron density was controlled by the magnitude and sign of the $z$-component of the electric field $E_z$ on the left boundary, which should have a minimum positive value $E_z \geq 0$, in accordance with the theory [8].

## 4. Mode of limitation of electron emission by the ion layer

To realize this mode, the following system parameters are set:

Potential of the right border is $U = 2$ kV; plasma source potential is $U_p = 30$ V;

Density components are $n_e \sim n_i = 10^9$ cm$^{-3}$;

Temperatures of the components are $T_e = 10$ eV; $T_i = 1$ eV; drift energy of ions is $w_B = 5$ eV.

The Debye length $l_D \sim 0.74$ mm is comparable with radius of emission aperture 1 mm. The solution time is 1 μsec, the number of macroparticles in the system is $N_i \sim 9 \cdot 10^4$, $N_e \sim 5 \cdot 10^4$.

When the system is filled with plasma, it shifts the equipotential lines to the cathode electrode (Fig.4*a*). At $r > 1.3$ mm, the potential decreases monotonically from 30 V to 0 over a length $l = 3$ mm from the left boundary to the cathode electrode. Note that the length of the segment is $l \sim 4l_D$, so that the entire gap on the plasma surface is a single Debye layer, in which the electron density drops to approximately $n \sim n_0 \exp(-l/l_D) \sim 0.02 n_0$.

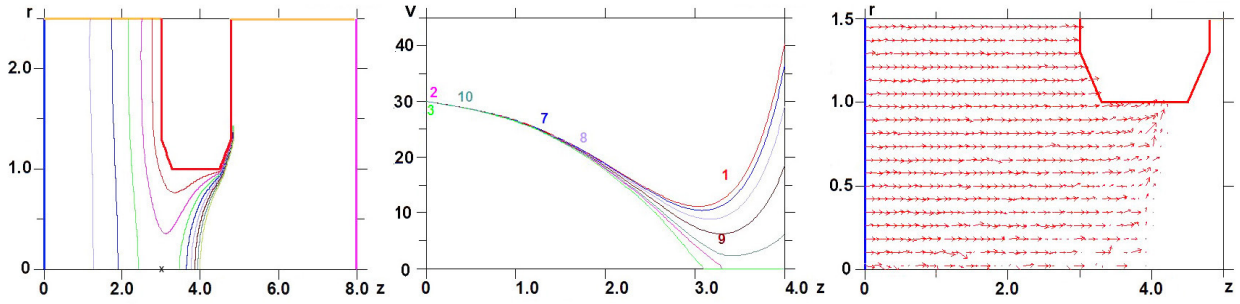


(a) (b) (c)

Fig.4. Equipotential curves, 5 V interval (*a*); $U(z)$ distribution at $r = 0.1$, 0.3, 0.5, 0.7, 0.9, 1.0, 1.2 mm (corresponded to curves 1, 7, 8, 9, 10, 2, and 3 from top to bottom) (*b*); ion current density distribution (*c*).

Since the Debye length is not small, the plasma in the aperture screens the electrode potential only partially. Near the axis, the potential distribution retains a saddle shape. On the axis, potential is minimal at the saddle point $z_s \sim 3$ mm, where $U_s \sim 11$ V. Here, the potential barrier for electrons is $w_e = e(U_p - U_s) \sim 19$ eV, which is ~1.2 times less than without plasma. The distribution of the potential along $z$ at different radii is shown in Fig.4*b*. As follows from it, the minimum barrier height changes insignificantly at $r \leq 0.3$ mm, increases to $w_e$ ~23 eV at $r = 0.5$ mm, and then increases along $r$, reaching 30 eV at the cathode electrode.

The distribution of ion fluxes is shown in Fig.4*c*. The ions leaving the plasma cross the minimum potential region and go to the cathode electrode. On the axis, their movement is approximately limited by an equipotential line $U = 35$ V, in accordance with their initial energy.

The electron density decreases towards the surface of the cathode electrode and towards the region of the emission aperture. The electrons that have overcome the potential barrier are further accelerated by the field towards the anode, forming a beam with a current $I_e \sim 6 \cdot 10^{-6}$ A. The distribution of the beam current density at the right boundary of the region $j_e(r)$ is characterized by a maximum current density of ~ 1 mA/cm$^2$ and a half-width of ~ 0.3 mm at half height. The root-mean-square angular velocity spread in the beam near the region boundary is ~ 0.08 rad, and is determined by the thermal electron velocities $(T_e/eU)^{1/2} \sim 0.08$ rad.

Thus, in this mode, the thermal electron emission $j_{0e}$ from the plasma is strongly limited by the potential barrier of the ion layer. This is the so-called regime of layered limitation of electron emission. For it, one can define the "transparency" of the cathode emission aperture as the ratio of

the output electron current $I_e$ through the aperture to the chaotic thermal current from the plasma source with the same area. The corresponding transparency factor $k$ is

$$k = I_e \Big/ \left( j_{0e} \cdot \pi r_0^2 \right) = I_e \left( 2m/\pi T_e \right)^{1/2} \Big/ \left( r_0^2 \cdot e \cdot n_0 \right) \sim 0.022, \tag{3}$$

where $r_0$ = 1 mm is the radius of the emission aperture, $j_{0e} = en_0(T_e/2\pi m)^{1/2}$ ~ 8.5 mA/cm$^2$ is the thermal current density in the unperturbed plasma. The value of the coefficient $k$ is due to both the current limitation by the barrier at $r$ ~ 0–0.1 mm and the effective decrease in the electron transmission area due to the potential barrier near the electrode.

## 5. Regime of a partially open plasma boundary

To obtain such a regime, the plasma density is increased by a factor of $10^2$, while the other system parameters are left the same.

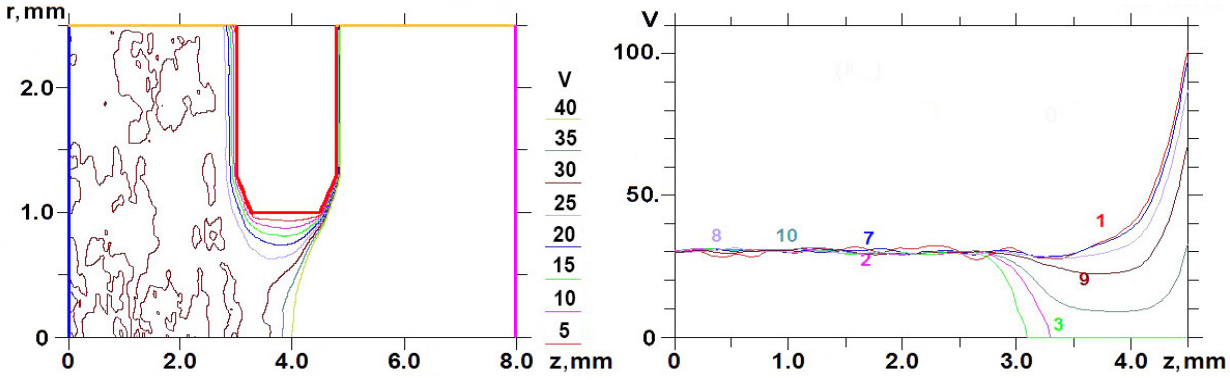


(a) (b)

Fig.5. Equipotentials $U(r,z)$ from 5 V to 40 V (*a*); $U(z)$ distribution, different radii as in Fig.4 (*b*)

Plasma density is $n_0 = 10^{11}$ cm$^{-3}$. The Debye length is reduced to $l_D$ ~ 7.4 $10^{-2}$ mm. The solution time is 900 ns, the number of macroparticles in the system is $N_i \sim 1.3 \cdot 10^5$, $N_e \sim 1.4 \cdot 10^5$.

The simulation results are shown in Fig.5. Here, the potential barrier near the axis of the emission aperture practically disappears. As can be seen in Fig.5*a*, filling the volume inside the cathode with plasma led to the displacement of equipotentials to the cathode electrode with the formation of an Debye layer with a thickness of ~ 0.3 mm. At $z$ < 2.8 mm, the potential is almost uniform, $U \sim U_p$, the electric fields and observed statistical fluctuations of the potential are small.

At $z$ > 2.8 mm, the character of the potential distribution along the $U(z)$ axis changes: at $r \leq 0.5$ mm, the potential exceeds the plasma potential, increasing towards the anode, $U > U_p$ (see Fig.5b), and there is no exit barrier for electrons. The thermal current density is $j_{0e}$ ~ 0.85 A/cm$^2$. In this region, electron emission occurs in the regime of an open plasma boundary. At $r$ > 0.5 mm the emission flux becomes limited. Already at $r$ = 0.7 mm, a potential pit to 22 V is observed, which corresponds to an electron barrier $w_e$ ~ 8 eV, which can lead to a significant decrease in the density of the emitted electron current. Towards the cathode electrode, the barrier increases to 30 eV, almost completely suppressing the emission.

The spatial distribution of the current densities of ions and electrons in the computational domain coincides qualitatively with the previous regime. The transparency coefficient increased by ~10 times, reaching $k = I_e/(j_{0e}\pi r_0^2) \sim 0.24$. The current density distribution along the right boundary is close to the previous one, but the maximum current density increased by a factor of $10^3$, up to 1.2 A/cm$^2$.

Thus, with a decrease in the Debye length a regime with a partially open plasma boundary is obtained. It is characterized by the fact that part of the plasma surface in the emission hole emits a thermal electron current that is not limited by the potential.

The change in the shape of the potential barrier during the transition from the regime of layered emission limitation to the regime of an open plasma boundary is shown in Fig.6. It shows the radial distribution profiles of the potential that limits electron flow through the emission aperture for plasma densities $n_0$ = $10^9$, $10^{10}$ and $10^{11}$ cm$^{-3}$ at a plasma potential $U_p$ = 30 V. The corresponding transparency coefficients are $k$ = 0.022, 0.056 and 0.24. As can be seen from the Fig.6, in case (*1*), the ion layers from the aperture edges overlap, forming a parabolic-type barrier profile. As the plasma density increases, the layer thickness decreases, and a potential "plateau" appears, which further declining and broadens along the radius with increasing potential gradient at the edges.

Let us estimate the transparency coefficient, similarly to [1, p.48, 50 etc.], assuming the distribution of electrons in terms of velocities to be Maxwellian, and in terms of potential to be Boltzmann:

$$k^* = en_0\sqrt{T_e/2\pi m}\cdot\int_0^{r_0}\exp(-e\varphi/T_e)\cdot 2\pi r dr\Big/\left(\pi r_0^2 j_{0e}\right), \qquad (4)$$

The coefficients calculated for the profiles in Fig.6 are $k^*$ = 0.1, 0.2, and 0.46, significantly differs from the values $k$ obtained by direct modeling. The reason is obvious – in the region of the barrier, through which a one way flow of electrons passes, their distribution differs greatly from both Maxwellian and Boltzmannian. Therefore, the approach [1] and expression (4) can be used only for a rough estimate.

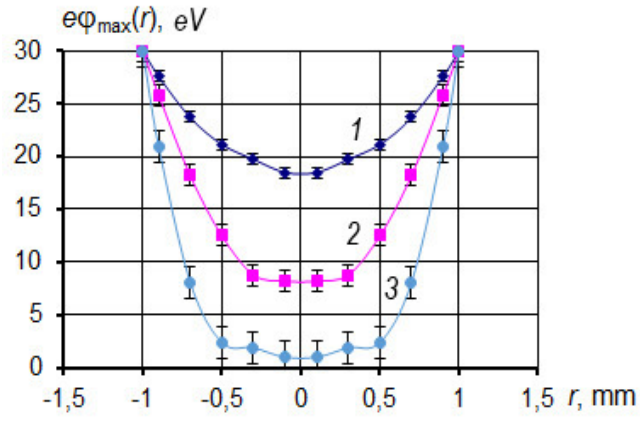


Fig.6. Distribution of the potential barrier along the radius at different plasma densities: $n_0$ = $10^9$ (*1*); $10^{10}$(*2*); $10^{11}$ cm$^{-3}$ (*3*).

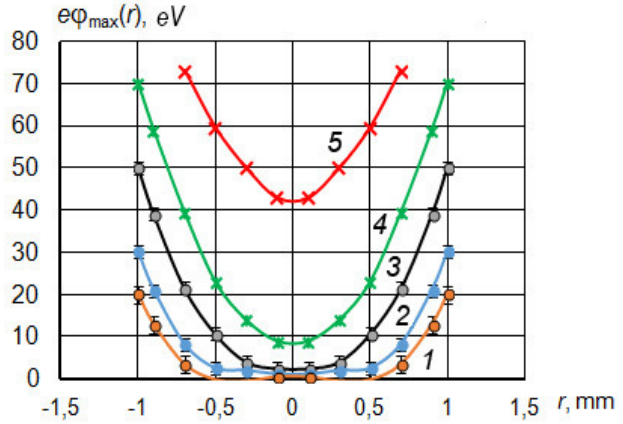


Fig.7. Barrier distribution in the aperture at different plasma potentials: $U_p$ = 20 (*1*); 30 (*2*); 50 (*3*); 70 (*4*); 100 V (*5*).

## 6. Effect of the plasma potential on electron emission

Above, the plasma potential $U_p$ was assumed to be constant, close to the floating plasma potential $\varphi_p$. Let us study the influence of the plasma potential on electron emission for the already considered regime with an open plasma boundary ($n_0$ = $10^{11}$ cm$^{-3}$, $U$ = 2 kV, $T_e$ = 10 eV, $T_i$ = 1 eV, $w_B$ = 5 eV, $l_D$ ~ 0.074 mm). For this, we consider the following values of the plasma potential: $U_p$ = 20, 30, 50, 70, and 100 V. The following are expected: a) a change in the energy of ions up to $eU_p$ + $w_B$, which can lead to a spatial redistribution of their density in the channel of the emission aperture and, accordingly, to a change in the configuration of electric fields affecting the emitted electron flux; b) the appearance of a "Langmuir additive" of the ion layer with an increase in $U_p$, that is, the

addition of a Langmuir layer between the Debye layer and the inner surface of the cathode, in which there are negligibly few electrons; c) change in the potential of the saddle point Us under the influence of these factors, so that the value of the potential barrier $e(U_p - U_s)$ can also change.

To analyze changes in the electron emission mode, Fig.7 shows the distribution profiles of the barrier potential in the region of the emission aperture. As can be seen, at the minimum plasma potential, the area of the open plasma boundary is maximum. With an increase in the potential near the floating one (up to $U_p = 50$ V), it narrows with an insignificant rise in the minimum value of $w_e$, which indicates the expansion of the near-electrode layer. Finally, at $U_p = 70$ V, the barrier increases to $w_e \sim T_e$, i.e., the open emission surface disappears, passing into the regime of layered emission limitation. With a further increase in the potential $U_p$, almost complete blocking of the emission occurs (Fig.8). Since the electron temperature and the unperturbed plasma density are conserved, it is clear that the expansion of the layer occurs due to the "Langmuir additive". It is impossible to calculate the thickness of the Langmuir layer using the “3/2 law”, since the conditions for its formation are not satisfied. In our case, ions enter the layer with initial energy $T_e/2e$ through a Debye layer of significant thickness in an electric field growing in the layer up to $\sim (8\pi n_0 T_e)^{1/2}$ and more [8]. In addition, the Debye length cannot be assumed to be conserved in the emission hole, since it assumes that the Boltzmann distribution of electrons is satisfied, which is absent under conditions of above-barrier emission (see the commentary on formula (4)). Therefore, numerical simulation seems to be the only way to calculate the profile of the ion layer and the coefficient of transparency of the emission aperture. The final dependence of the transparency coefficient $k$ on the plasma potential is shown in Fig.8.

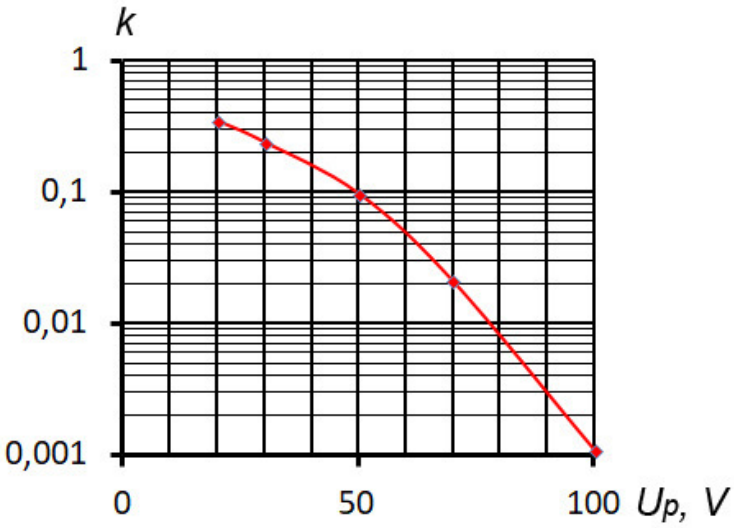


Fig.8. Dependence of the transparency coefficient of the emission aperture on the plasma potential.

## 7. Conclusion

Numerical simulation of the plasma emitter of electrons operation for the real diode geometry has been carried out. When modeling a section of a separate cell of a multi-aperture electron beam by the PIC method, the regime of electron emission from a partially open plasma boundary and the regime of layered emission limitation were obtained. The dependences of the emission characteristics on the density and potential of the emitting cathode plasma during transitions between regimes are quantitatively studied. For them, the profiles of the potential barrier, the coefficient of their transparency for electrons in the emission hole, and the characteristics of the formed electron beam were obtained. The necessity of using numerical simulation to analyze the

operation of the electron emitter instead of estimates using the Maxwellian and Boltzmann distributions is shown.

**Acknowledgement**

The work was supported by the Ministry of Science and Higher Education of the Russian Federation.

**8. References**

[1] Oks E.M., *Electron Sourses with Plasma Cathode: Physics, Technics, Applications (*in Russian*)*. (Tomsk: Publishing House, 2005).
[2] Boers J.E. *Proc. Int. Conf. on Part. Acc.*, *Washington, DC, USA*, **1**, 327, 1993; doi: 10.1109/PAC.1993.308924
[3] Spädtke P., Muehle C., *Rev. Sci. Instr.*, **71**(2), 820, 2000; doi: 10.1063/1.1150303
[4] Petrovich O.N., Gruzdev V.A. *Appl. Phys., (in Russian),* **2**, 79, 2012.
[5] Astrelin V.T. *Advance Appl. Phys., (in Russian),* **1**(5), 571, 2013; url: https://advance.orion-ir.ru/UPF-13/5/UPF-1-5-574.pdf
[6] Tarakanov V.P., *Mathematical Simulation: Problems and Results, (in Russian).* (Moscow: Nauka, 2003).
[7] Kurkuchekov V.V., *Spatial and angular characteristics of an electron beam obtained in a multi-aperture source with a plasma emitter, PhD thesis*, *(in Russian)*. (Novosibirsk: Budker Institute of Nuclear Physics, 2020).
[8] Kotelnikov I.A., Astrelin V.T., *Physics-Uspekhi*, 2015, **58**(7), 701, 2015; doi: 10.3367/UFNe.0185.201507c.0753